EARTHQUAKE SPECTRA

Earthquake Spectra
1–24

DOI: 10.1177/8755293019899950
journals.sagepub.com/home/eqs
SAGE

A database of test results from steel and reinforced concrete infilled frame experiments

Honglan Huang, M.EERI and Henry V Burton, M.EERI

Abstract

Extensive experimental investigations into the behavior of reinforcement concrete and steel frames with infill have been conducted worldwide. However, there are very few systematically created and publicly available databases on infilled frame experiments. This article assembles a database of 264 experiments on single-story infilled frames, which includes specimens with different types of frames and panels. It has been utilized by the authors (in separate studies) to develop (1) empirical equations for modeling the infill panels as equivalent struts and (2) machine learning models for failure mode classification. The intent is for the database to be augmented and further used in various other applications in studying the seismic behavior of masonry-infilled frames.

Keywords

Database, masonry-infilled frame, numerical modeling, empirical model, backbone curve

Date received: 16 December 2019; accepted: 16 December 2019

Introduction

Masonry infill panels are commonly used as non-structural walls and partitions in reinforced concrete (RC) and steel frame buildings (Shing and Mehrabi, 2002). Extensive studies have been carried out to investigate the seismic behavior of masonry-infilled frames, especially the influence of frame–infill interaction on overall structural performance (Asteris et al., 2011; Liberatore et al., 2017; Noh et al., 2017). However, the design and assessment of infilled frame structures remains a challenging task. To enable the implementation of the performance-based earthquake engineering (PBEE) framework for seismic risk assessment of infilled frames, reliable numerical models are needed to simulate the full range of the nonlinear behavior from the onset of damage through collapse (Haselton

Department of Civil and Environmental Engineering, University of California–Los Angeles, Los Angeles, CA, USA

Corresponding author:
Honglan Huang, Department of Civil and Environmental Engineering, University of California–Los Angeles, Los Angeles, CA 90095, USA.
Email: honglanhuang@ucla.edu

et al., 2008; Koliou and Filiatrault, 2017; Lignos, 2008). The development of such numerical models requires reasonably simplified representations of the structure as well as reliable estimates of the parameters that characterize the nonlinear behavior. Both of these aspects rely on calibration and validation using adequate data from physical experiments.

Experimental databases for various types of structural components have been developed and are publicly available to enable nonlinear modeling and analysis. Such databases have been developed for steel frame members (Lignos and Krawinkler, 2011), RC columns (Berry et al., 2004), and wood and steel diaphragm connectors (Koliou and Filiatrault, 2017). Experimental investigations of infilled RC and steel frames have been performed worldwide. However, there are several challenges to the development of an infilled frame database: the data from these experiments exist in various sources, such as journal papers, conference proceedings, and technical reports; the programs were carried out in different countries and time-periods, resulting in different design methodologies, test setups, characteristic parameters, and the associated notations and units, and the standards for reporting and classifying failure modes. Recently, several studies have made efforts to develop databases for infilled frame experiments. Liberatore et al. (2017) assembled a database of 116 masonry-infilled RC frames, 7 masonry-infilled steel frames, and 39 confined masonry specimens and used them to assess and modify a series of analytical equations for characterizing the in-plane response of infilled frames. In the supplementary material, they provided a table with metadata and structural properties (with varying levels of detail) from each experiment and an excel spreadsheet with the parameters computed using their proposed equations. Luca et al. (2016) compiled a database of 101 masonry-infilled RC frames, which includes the testing protocol, structural properties, and piecewise linear backbone curves, and the damage to the specimens was classified using a previously developed standard. Several studies assembled infilled frame databases and used them to develop drift-based empirical fragility functions for in-plane response. Examples include the ones by Cardone and Perrone (2015), Sassun et al. (2016), and Chiozzi and Miranda (2017), which contain 55, 50, and 152 specimens, respectively. De Risi et al. (2018) assembled a database of 219 specimens, focusing on damage assessment of RC frames with unreinforced hollow clay brick panels. These studies provide diverse sets of valuable information on experimental investigations of infilled frames. However, to date, only Liberatore et al. (2017) provided public access to their electronic data.

The database presented in this article consists of 264 infilled frame specimens, including 191 constructed with RC frames and 73 constructed with steel frames. The intent is to contribute toward (1) the improvement of nonlinear analysis models for characterizing seismic behavior, (2) the development of empirical predictive models for estimating the characteristic parameters in various analysis models, and (3) the understanding and systematic classification of the failure modes in infilled frame structures. The data were assembled from 49 journal publications, conference proceedings, and technical reports. A broad range of infill panel types are included, and unified parameters and notations for the attributes of data are adopted. Information contained in the database includes the metadata from each experiment, the structural properties of the infilled frame components, and the experimental results (force–displacement curves), as made available in the relevant source. The database (Huang and Burton, 2019b) is accessible electronically on the DesignSafe cyberinfrastructure (Rathje et al., 2017). A subset of the database has been used to calibrate parameters for a pinched hysteretic material model for infill struts used to model RC infilled frames (Huang et al., 2019). In this study, a set of empirical equations were developed for describing the relationship between the backbone curve parameters and the

properties of the infill panel. A subset of the database has also been used to develop a machine learning model to classify the in-plane failure modes of RC infilled frames (Huang and Burton, 2019a). Such models are able to predict the mode of in-plane failure (e.g. shear sliding of the infill and column flexural hinging; shear sliding of the infill and column shear failure) given the properties of the infilled frame. This data article provides details of the key aspects of the database and statistical summaries of important parameters.

Summary and sources used to develop the database

The infilled frame database is collected from experimental investigations reported in 49 journal publications, conference proceedings, and technical reports, which are summarized in Table 1. The information included in the database can be categorized as follows:

1. *Metadata*: general information about each test specimen, including details about the frame, the type of masonry unit used, whether there are openings in the infill panel, and loading protocols.
2. *Structural properties*: the geometric and material properties of the frame and infill, the reinforcement details of concrete frames, and the section sizes.
3. *Experimental results*: the hysteretic curves from each experiment (if provided by the original authors), which have been extracted using a digitization software, are made available in .csv format.

Metadata

The data attributes contained in the metadata are listed in Table 2 along with a brief description for each one. Three types of information are included in the metadata: (1) *Test*, which provides the references and identifying information associated with each test specimen; (2) *General information*, which includes characteristics of the frame and infill panel; and (3) *Loading information*, which documents the lateral and vertical loading used in each test.

The entire database consists of 257 one-bay one-story and 7 multi-bay one-story masonry-infilled frames. A total of 191 RC frames and 73 steel frames are included, which are recorded in separate excel sheets. The infill panels include a range of different types of masonry units, reinforced and unreinforced masonry, panels with and without opening, and with and without retrofit measures. Figure 1 presents a graphical summary of the types of infill frames included in the database.

Structural properties

This section describes the data collected on the structural properties of the test specimens. The properties are organized as geometric and material properties of the frame (depending on whether it is RC frame or steel frame), the reinforcing details of the concrete frame, and the geometric and material properties of the infill panel. All the properties are converted to U.S. customary units.

Table 1. Database sources

Reference	Number of specimens	Frame type	Loading type
Abdul-kadir (1974)	12	Steel	Monotonic
Akhoundi et al. (2018)	1	RC	Quasi-static cyclic
Al-Chaar et al. (2002)	4	RC	Monotonic
Angel et al. (1994)	7	RC	Quasi-static cyclic
Anil and Altin (2007)	7	RC	Quasi-static cyclic
Baran and Sevil (2010)	3	RC	Quasi-static cyclic
Basha and Kaushik (2016)	9	RC	Quasi-static cyclic
Bergami and Nuti (2015)	2	RC	Quasi-static cyclic
Billington et al. (2009)	1	RC	Quasi-static cyclic
Blackard et al. (2009)	4	RC	Quasi-static cyclic
Bose and Rai (2014)	1	RC	Quasi-static cyclic
Calvi and Bolognini (2008)	4	RC	Quasi-static cyclic
Campione et al. (2014)	12	RC	Quasi-static cyclic
Chiou and Hwang (2015)	4	RC	Quasi-static cyclic
Colangelo (2005)	11	RC	Pseudo-dynamic
Combescure et al. (1996)	2	RC	Quasi-static cyclic
Crisafulli (1997)	2	RC	Quasi-static cyclic
Da Porto et al. (2013)	6	RC	Quasi-static cyclic
Dautaj et al. (2018)	7	RC	Quasi-static cyclic
Dawe and Seah (1989)	28	Steel	Monotonic
Fiorato et al. (1970)	7	RC	Monotonic
Flanagan and Bennett (1999)	8	Steel	Quasi-static cyclic
Gazic and Sigmund (2016)	11	RC	Quasi-static cyclic
Haider (1995)	4	RC	Quasi-static cyclic
Kakaletsis and Karayannis (2008)	6	RC	Quasi-static cyclic
Khoshnoud and Marsono (2016)	2	RC	Monotonic
Kumar et al. (2016)	1	RC	Quasi-static cyclic
Leuchars and Scrivener (1976)	2	RC	Quasi-static cyclic
Liu and Soon (2012)	10	Steel	Monotonic
Mansouri et al. (2014)	5	RC	Quasi-static cyclic
Markulak et al. (2013)	6	Steel	Quasi-static cyclic
Mehrabi et al. (1996)	10	RC	Monotonic/Quasi-static cyclic
Misir et al. (2015)	5	RC	Quasi-static cyclic
Morandi and Magenes (2014)	4	RC	Quasi-static cyclic
Mosalam et al. (1997)	4	Steel	Quasi-static cyclic
Pires et al. (1997)	2	RC	Quasi-static cyclic
Schwarz et al. (2015)	3	RC	Quasi-static cyclic
Sigmund and Penava (2013)	9	RC	Quasi-static cyclic
Stylianidis (2012)	5	RC	Quasi-static cyclic
Tasnimi and Mohebkhah (2011)	5	Steel	Quasi-static cyclic
Tawfik Essa et al. (2014)	3	RC	Quasi-static cyclic
Tizapa (2009)	3	RC	Quasi-static cyclic
Verderame et al. (2016)	2	RC	Quasi-static cyclic
Waly (2010)	2	RC	Quasi-static cyclic
Yorulmaz and Sozen (1968)	7	RC	Monotonic
Yuksel and Teymur (2011)	2	RC	Quasi-static cyclic
Zarnic and Tomazevic (1985)	3	RC	Quasi-static cyclic
Zhai et al. (2016)	3	RC	Quasi-static cyclic
Zovkic et al. (2013)	3	RC	Quasi-static cyclic

RC: reinforced concrete.

Table 2. Metadata

	Attribute	Description
Test	ID	An ID number used to identify the specimen in the database
	Reference	The source paper/report of the experiment
	Specimen	Name of the specimen in the source paper/report
General information	Scale	Scale of the test specimen
	Note on frame	A short note on the frame
	No. of bays	No. of bays of the frame
	Masonry type	Type of masonry used for the infill panel
	Retrofit status	Whether the specimen has been repaired or retrofitted
	Panel reinforcing status	Whether the infill panel is reinforced
	Panel reinforcement description	Description on the panel reinforcement if applicable
	Frame–panel interface connection	Whether there are shear connections at the frame–panel interface
	Frame–panel interface details	Details of the frame–panel interface (e.g. type of shear connection, size of gap), where applicable
	Panel opening	Whether the panel has an opening
Loading information	Lateral loading type	Type of lateral loading
	Vertical load location	Location of the applied vertical load
	P	Value of the applied vertical load (kips), all converted to concentrated load

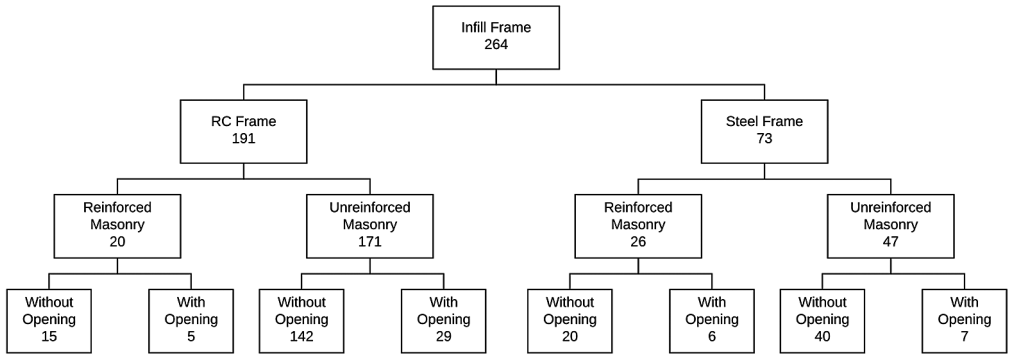

Figure 1. Summary of the specimen types included in the database.

Geometric properties of the RC frames. The geometric properties provided for RC frames are listed in Table 3, which include the story height and span of the bay (centerline dimensions) and the cross-sectional properties of the beam and column.

Material properties of the RC frames. Table 4 lists the material properties of the RC frames recorded in the database. For specimens where the modulus of elasticity of the frame concrete is not provided in the source paper/report, the empirical equation recommended by ACI-318-14 (ACI Committee 318, 2014) is used to calculate the corresponding value:

Table 3. Geometric properties of the reinforced concrete frame

	Property notation	Description	Unit
Frame	H	Story height of the frame, measured to the centerline of the beams	in
	L	Span of each frame bay, measured to the centerline of the columns	in
Beam	b	Width of the cross section	in
	h	Total depth of the cross section	in
	A_g	Gross area of the cross section	in^2
	I_x	Moment of inertia about the x–x axis of the cross section	in^4
Column	b	Width of the cross section (perpendicular to the applied lateral load)	in
	h	Total depth of the cross section (parallel to the applied lateral load)	in
	A_g	Gross area of the cross section	in^2
	I_x	Moment of inertia about the x–x axis of the cross section	in^4

Table 4. Material properties of the reinforced concrete frame

Material	Property notation	Description	Unit
Concrete	f'_c	Concrete compressive strength	$kips/in^2$
	E_c	Concrete modulus of elasticity	$kips/in^2$
Steel reinforcement	f_{yl}	Yield strength of the longitudinal reinforcement	$kips/in^2$
	f_{yt}	Yield strength of the transverse reinforcement	$kips/in^2$

$$E_c = 57,000\sqrt{f'_c} \tag{1}$$

where E_c is the modulus of elasticity of the frame concrete and f'_c is the compressive strength of the concrete—both terms are in units of pounds and inches (specifically when using Equation 1).

Reinforcing details for the concrete frames. The geometric properties of the concrete frame reinforcement are listed in Table 5. The collection, organization, and notation of these properties are consistent with that of Haselton et al. (2008), who developed a set of empirical equations to predict the modeling parameters of beam–column elements used in the nonlinear analysis of RC frames.

It should be noted that the values of clear cover to the rebar are not reported in many of the data sources. Therefore, most of the recorded values of the distance from the center of the compression reinforcement to the extreme compression fiber (d'), and the effective depth of the cross section (d), are measured directly from the figures showing cross-section reinforcing details in the corresponding paper/reports (see Figure 2). The accuracy of these recorded values might vary. It is recommended that when calculating the reinforcement ratio, assumptions deemed reasonable by the users can be applied to estimate the effective depth.

Geometric properties of the steel frames. Table 6 lists the geometric properties of the steel frame members. All notations for the steel section properties are in accordance with ASTM specifications (ASTM A6/A6M-17a, 2017). Figure 3 shows the cross section of the wide-flange steel member.

Table 5. Reinforcing properties

Component	Property notation	Description	Unit
Beam	$d_{b,l}$	Diameter of longitudinal bars	in
	d'	Distance from the center of compression reinforcement to the extreme compression fiber	in
	d	Effective depth of the cross section	in
	$A_{s,top}$	Total area of top longitudinal reinforcement in the cross section	in^2
	$\rho_{l,top}$	Ratio of the top longitudinal reinforcement area to that of the effective cross section ($A_{s,top}/bd$)	
	$A_{s,bot}$	Total area of the bottom longitudinal reinforcement	in^2
	$\rho_{l,bot}$	Ratio of the bottom longitudinal reinforcement area to that of the effective cross section ($A_{s,bot}/bd$)	
	$A_{s,total}$	Total area of the longitudinal reinforcement in the cross section	in^2
	$\rho_{l,total}$	Ratio of the total longitudinal reinforcement area to that of the effective cross section ($A_{s,total}/bd$)	
	$d_{b,t}$	Diameter of the transverse reinforcing bars	in
	s	Spacing of the transverse reinforcement, at the end region (close spacing)	in
	ρ_t	Transverse reinforcement ratio at the end region (close spacing) of the beam (in most cases (two-legged stirrup), calculated by $2(\frac{\pi d_{b,t}^2}{4})/bs$)	
Column	$d_{b,l}$	Diameter of the longitudinal reinforcing bars	in
	$A_{s,total}$	Total area of longitudinal reinforcement in the cross section	in^2
	$\rho_{l,g}$	Ratio of the total longitudinal reinforcement area to that of the gross cross section ($A_{s,total}/A_g$)	
	$d_{b,t}$	Diameter of the transverse reinforcing bars	in
	s	Spacing of the transverse reinforcement at the end region (close spacing)	in
	ρ_t	Transverse reinforcement ratio at the end region (close spacing) of the column (in most cases (two-legged stirrup), calculated by $2(\frac{\pi d_{b,t}^2}{4})/bs$)	

Material properties of the steel frames. Where available, the yield and ultimate strength (very few available) of the steel frame members are provided (see Table 7).

Geometric properties of the infill panels. As noted in the beginning of "Summary and sources used to develop the database" section, the database incorporates infilled frames with and without panel openings. The geometric properties of the panel and opening are listed in Table 8. Three measurements are used to document the location and size of the opening: the length (l_0) and height of the opening (h_0) and the ratio between the distance from the center of the opening to the left boundary of the infill panel and the length of the panel (x/l_w). Figure 4 shows the key geometric parameters of the frame, panel, and opening.

Material properties for the infill panel. The material properties for the infill panel are listed in Table 9. The compressive strength of the masonry prism (f'_m) was provided for most of the specimens and is based on compressive tests with the loading applied perpendicular to the bed joints. Where the modulus of elasticity of the masonry prism (E_m) is not provided, the

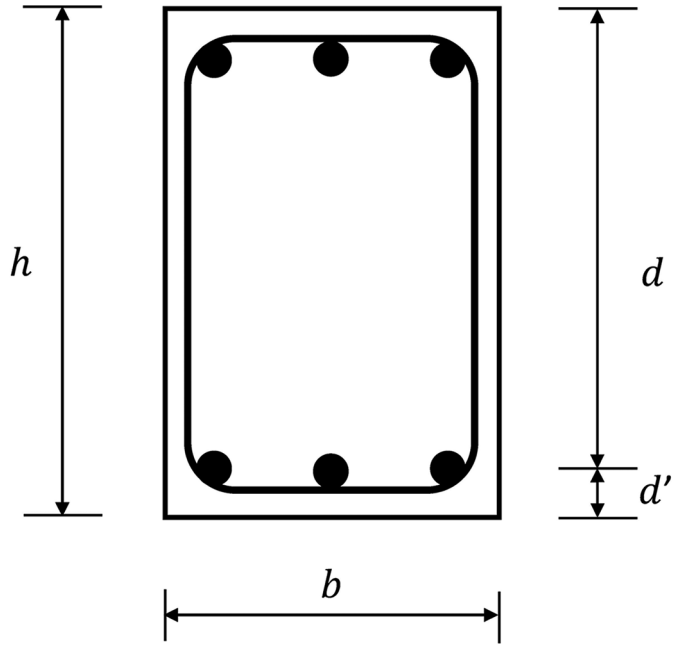

Figure 2. Cross section of an RC beam.

Table 6. Geometric properties of the steel frame

Component	Property notation	Description	Unit
Frame	H	Story height measured to the centerline of the beams	in
	L	Bay width measured to the centerline of the columns	in
Beam and column	Shape	Shape of the steel section	
	A_g	Gross area of the cross section	in^2
	h	Total depth of the cross section	in
	b	Width of the flange	in
	t_f	Thickness of the flange	in
	w	Thickness of the web	in
	I_x	Moment of inertia about the x–x axis	in
	r_x	Radius of gyration about the x–x axis	in
	I_y	Moment of inertia about the y–y axis	in
	r_y	Radius of gyration about the y–y axis	in

empirical equation proposed by Kaushik et al. (2007) and recommended by FEMA 306 (2000) is used to calculate E_m:

$$E_m = 550 f'_m \tag{2}$$

The compressive strength of the masonry units (f_b), mortar (f_{mortar}), and the cohesion of the brick–mortar interface (τ_0) are only available for a small portion of the specimens.

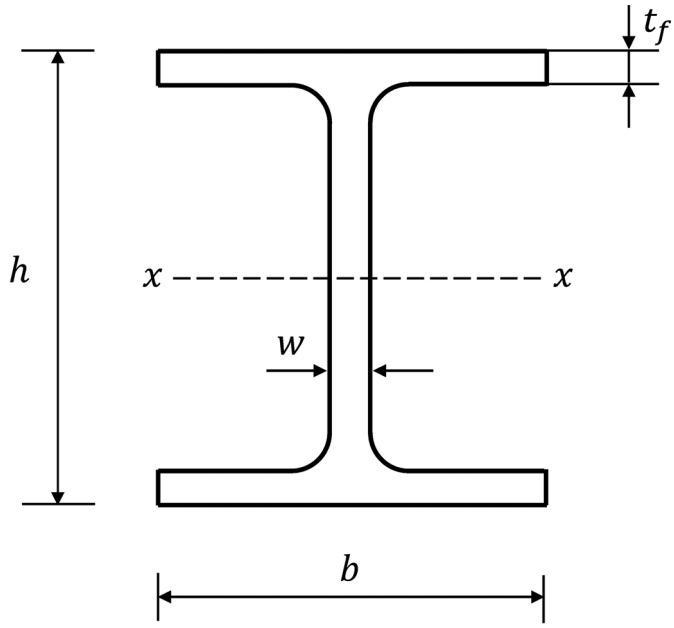

Figure 3. Cross section of a typical wide-flange steel member.

Table 7. Material properties of the steel frame members

Property notation	Description	Unit
F_y	Yield strength	kips/in^2
F_u	Ultimate strength	kips/in^2

Table 8. Geometric properties of the infill panel

	Property notation	Description	Unit
Panel	h_w	Height of the infill panel	in
	l_w	Length of the infill panel	in
	t_w	Thickness of the infill panel	in
Opening	l_0	Length of the opening in the infill panel	in
	h_0	Height of the opening in the infill panel	in
	x/l_w	Ratio between the distance from the center of the opening to the left boundary to the length of the infill panel	in

Force–displacement curve

A force–displacement curve provides information on the nonlinear response history of the test specimens under monotonic, cyclic, or dynamic loading, which is critical for analyzing the overall behavior, calibrating numerical model parameters, and developing analytical equations for response estimation. However, there are several challenges associated with acquiring the force–displacement data. Several sources did not provide the force–

Table 9. Material properties of the infill panel

Property notation	Description	Units
f_b	Compressive strength of the masonry unit	kips/in^2
f_{mortar}	Compressive strength of the mortar	kips/in^2
f'_m	Compressive strength of the masonry prism	kips/in^2
E_m	Modulus of elasticity of the masonry prism	kips/in^2
τ_0	Cohesion of the brick–mortar interface, which is equal to the shear strength under zero axial stress	kips/in^2

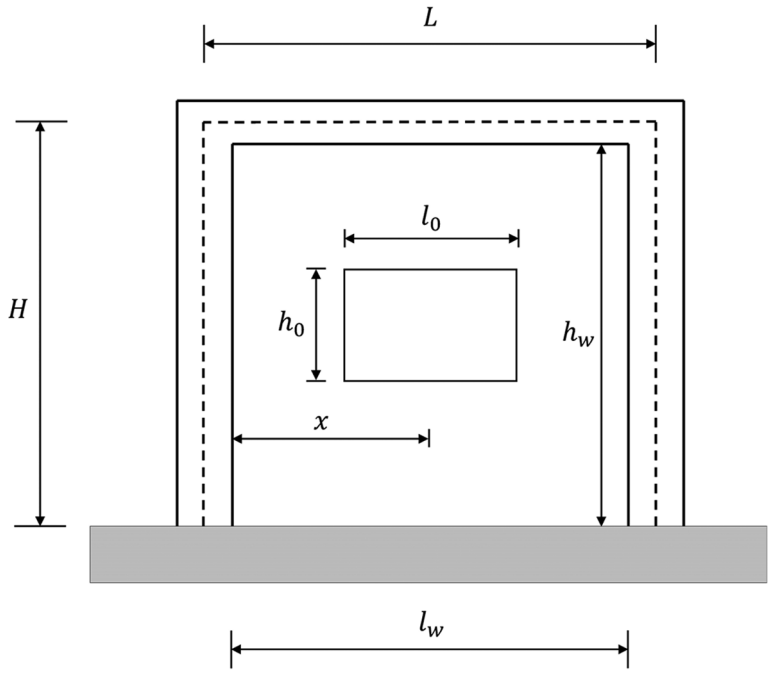

Figure 4. Geometry of the infilled frame.

displacement curves for all the specimens tested. Moreover, in many cases, the provided force–displacement curves are only available graphically instead of in the original digital format.

In order to extract key response parameters from the force–displacement curves, the authors converted the plot images to digital format. However, for cyclically loaded specimens, the sequences of the original hysteretic cycles cannot be inferred from the digitized data. In other words, the plotted figure can reproduce the curve visually but the information about the sequence of the load–displacement cycles cannot be extracted. Therefore, such data can inform visual calibration but not energy-based analysis. However, we were able to extract the envelope curves from the digitized data, which is ordered from the largest negative displacement to the largest positive displacement.

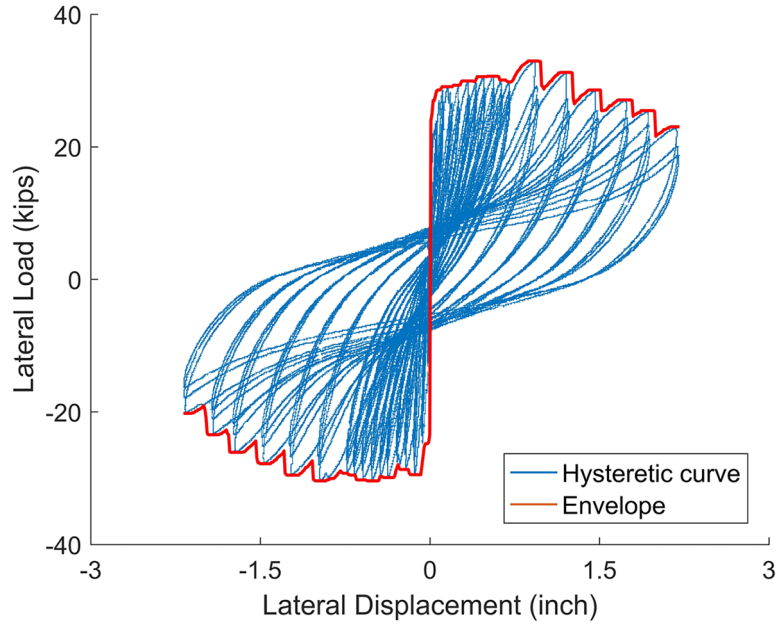

Figure 5. Force–displacement hysteretic curve and envelope.

The database provides the force–displacement data (in comma-separated (.csv) format) for test specimens where such information is available in the source paper/report, as well as the envelope curves for cyclically loaded specimens. The first column in the .csv file records the displacement values, and the second column has the corresponding force values. Figure 5 shows an example of the plotted force–displacement and envelope curve data for the test specimen in the experimental program by Bose and Rai (2014).

Statistical summary of the structural properties

This section provides a statistical summary of the data in the structural property category. All notations and units correspond to those described in the previous section.

RC frame

The distributions of key properties of the RC frame and the components (beam and column) for the 191 specimens are presented in Figures 6 to 8 as histograms. The story heights range from 16.50 to 123.03 in, with a mean of 62.92 in (5.24 ft). Approximately 70% of the specimens have a story height in the range of 50 in (4.17 ft) to 100 in (8.33 ft). Approximately 50% of the test specimens have a concrete compressive strength f_c' between 3 and 5 ksi.

The distributions of key properties of the RC column are presented in Figure 8. The axial load ratio ($P/A_g f_c'$) ranges from 0 to 0.37, and 31% of the specimens were tested with no axial load. The transverse reinforcement ratio ranges from 0.0007 to 0.0168, and 57.4% of the test specimens have a column transverse reinforcement ratio that is less than 0.05,

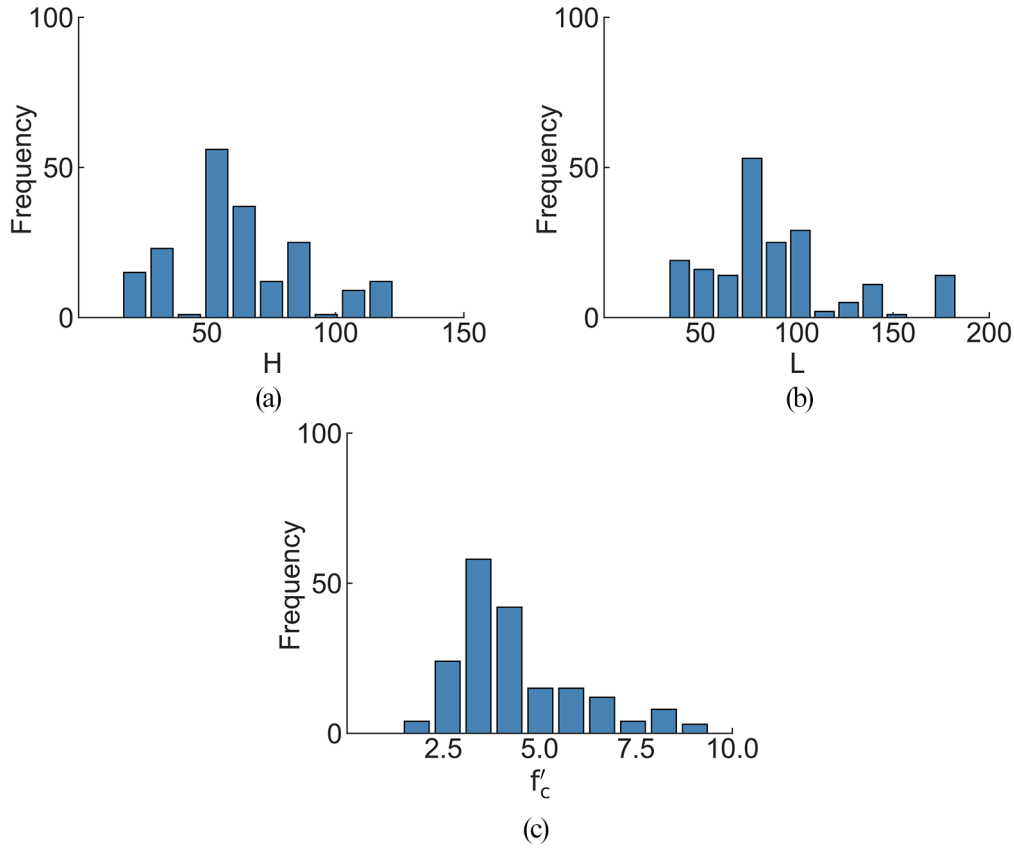

Figure 6. Distribution of the RC frame properties: (a) H, (b) L, and (c) f_c'.

indicating non-ductile detailing, which is typical for many existing RC infilled frame buildings.

Steel frame

The distribution of the key properties for the steel frame and its components (beam and column) for 73 specimens are shown in Figures 9 to 11. The story height of the steel frame specimens ranges from 16.3 in (1.36 ft) to 115.7 in (9.64 ft). Among the 45 specimens for which the yield strength of steel (F_y) is provided, the F_y value ranges from 36 to 54.1 ksi, with 86.7% (39/45) greater than 45 ksi.

Masonry infill panel

The distributions of key geometric and material properties for the infill panel in the 264 test specimens are shown in Figure 12. Here, 76% of the specimens have an aspect ratio (h_w/l_w) between 0.5 and 1.0. Only five "slender" specimens are included with aspect ratios of approximately 1.5. The masonry prism strength ranges from 0.12 to 5.13 ksi, with a mean of 1.64 ksi. More than 50% of the test specimens have a prism strength lower than 1.0 ksi.

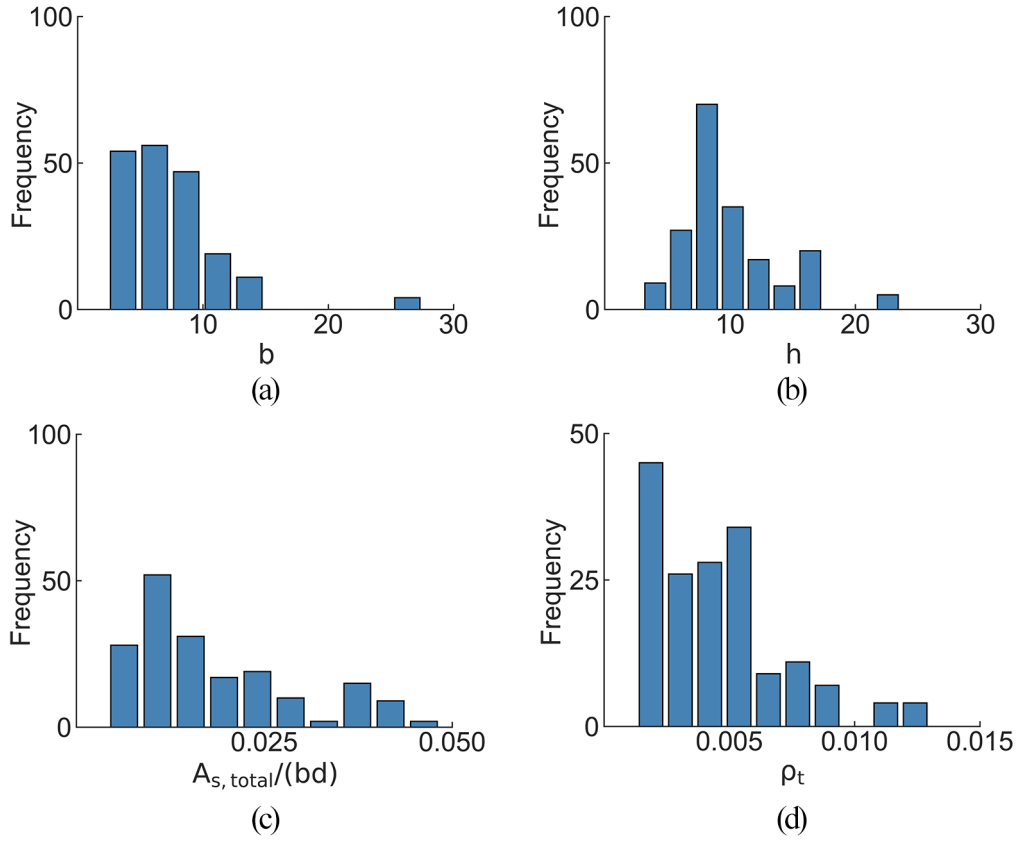

Figure 7. Distribution of the RC beam properties: (a) b, (b) h, (c) $A_{s,\,total}/(bd)$, and (d) ρ_t.

Figure 13 shows the distribution of panel opening geometries for 45 specimens. Here, 66.7% of the specimens have openings located at the center of the panel, while 33.3% have openings located away from the center of the panel.

Summary of prior applications of the database

A subset of the developed database was utilized in a study by the authors to develop empirical equations for the backbone curve parameters that characterize the nonlinear response of infill panels modeled as equivalent diagonal struts (Huang et al., 2019). The dataset utilized in that study consists of 113 specimens that are constructed using RC frames with unreinforced masonry panels without openings or retrofit measures. The RC beams and columns are represented using a concentrated plasticity model consisting of elastic beam–column elements with two zero-length hinges at the ends. The beam hinge is modeled using a flexural spring with the peak-oriented hysteretic model developed by Ibarra et al. (2005), and the column hinge is modeled with two springs in series: a flexural spring with the peak-oriented hysteretic material model (Ibarra et al., 2005) and a shear spring with the shear failure model (*LimitState* material model) developed by Elwood (2004). The infill panel is modeled with two diagonal struts (one in each direction) using a

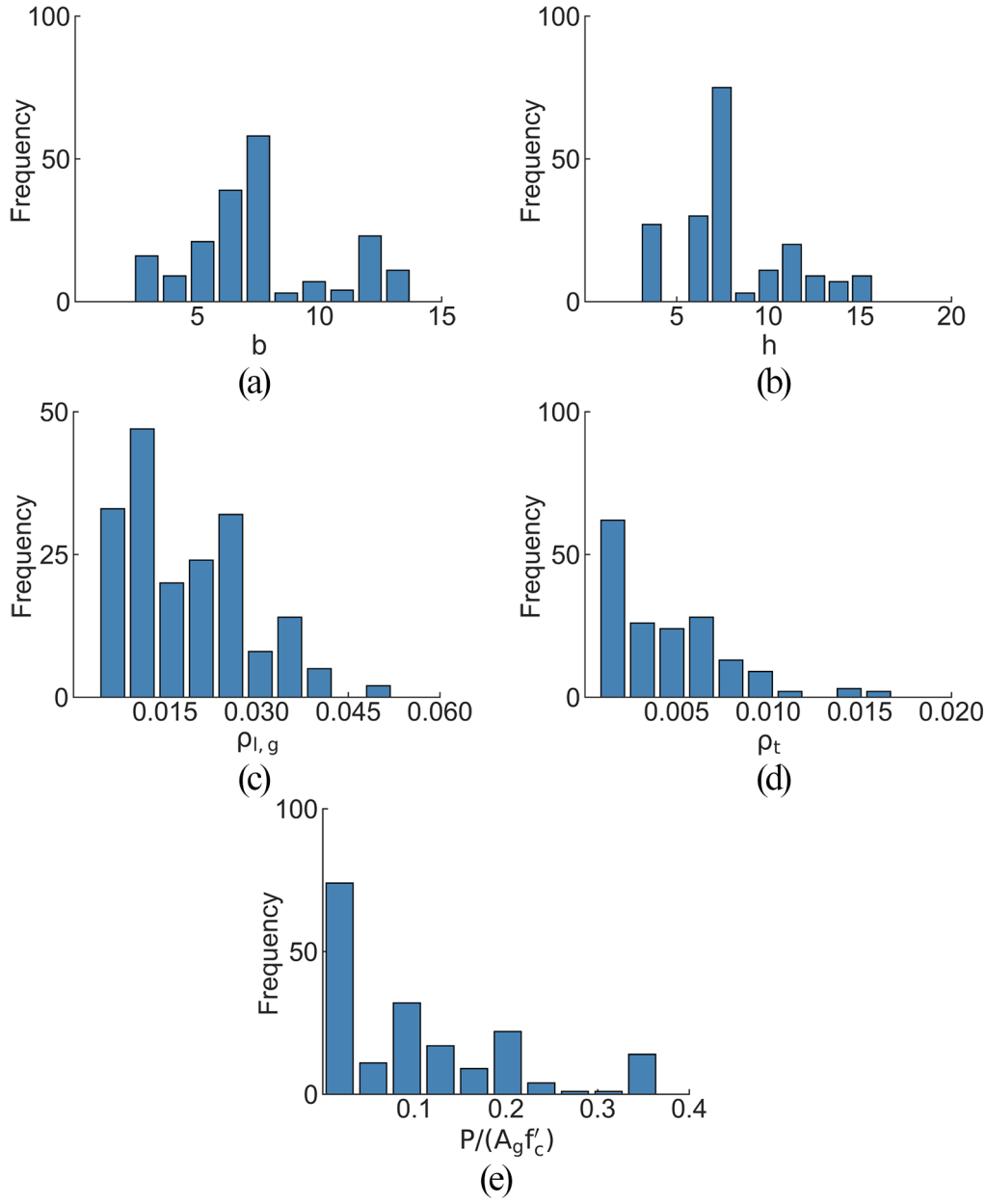

Figure 8. Distribution of the RC column properties: (a) b, (b) h, (c) $\rho_{l,g}$, (d) ρ_t, and (e) $P/(A_g f'_c)$.

truss (axial-only) element with the *Pinching4* material model developed by Lowes et al. (2004) in the Open System for Earthquake Engineering Simulation (McKenna et al., 2000).

The parameters of the *Pinching4* material for the infill struts are calibrated iteratively by seeking a visual match between the experimental hysteretic curve of the entire infilled frame and the hysteretic curve from the numerical analyses in OpenSees. Further details of

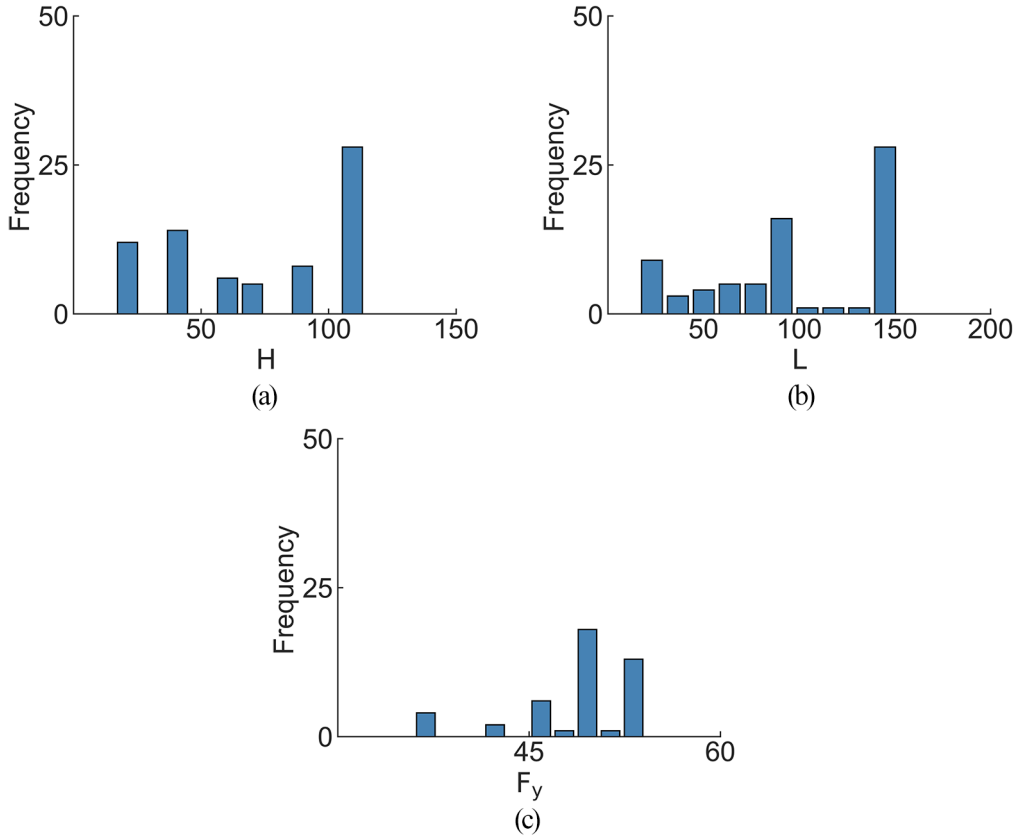

Figure 9. Distribution of the steel frame properties: (a) *H*, (b) *L*, and (c) F_y.

the assumptions used to calibrate the *Pinching4* parameters can be found in Huang et al. (2019). Some of these modeling assumptions are based on the paper by Noh et al. (2017), which provides a comprehensive review and assessment of the numerical modeling methods for infilled frames. For illustration, we again use the test specimen in the experimental program by Bose and Rai (2014) as an example. Additional specimen calibrations can be found in Huang et al. (2019). Figure 14 shows the result of the calibration, where the blue solid line represents the experimental hysteretic curve and the brown dashed line represents the response simulated using the OpenSees model.

The developed empirical equations for the backbone curve parameters for the axial response of the equivalent infill struts are listed in Table 10 (in U.S. customary units). The parameters are based on the *Pinching4* material but are adaptable to other similar models.

Another subset of the dataset comprising 114 RC infilled frame specimens without openings was used to develop machine learning models to classify their in-plane failure modes (Huang and Burton, 2019a). To obtain the learning labels, the four distinct in-plane failure modes described by Tempestti and Stavridis (2017) were adopted (their proposed classification rule based on two quantitative metrics was not used). The labels were assigned by classifying the observed and documented failure mechanism from each experiment based on the following categories:

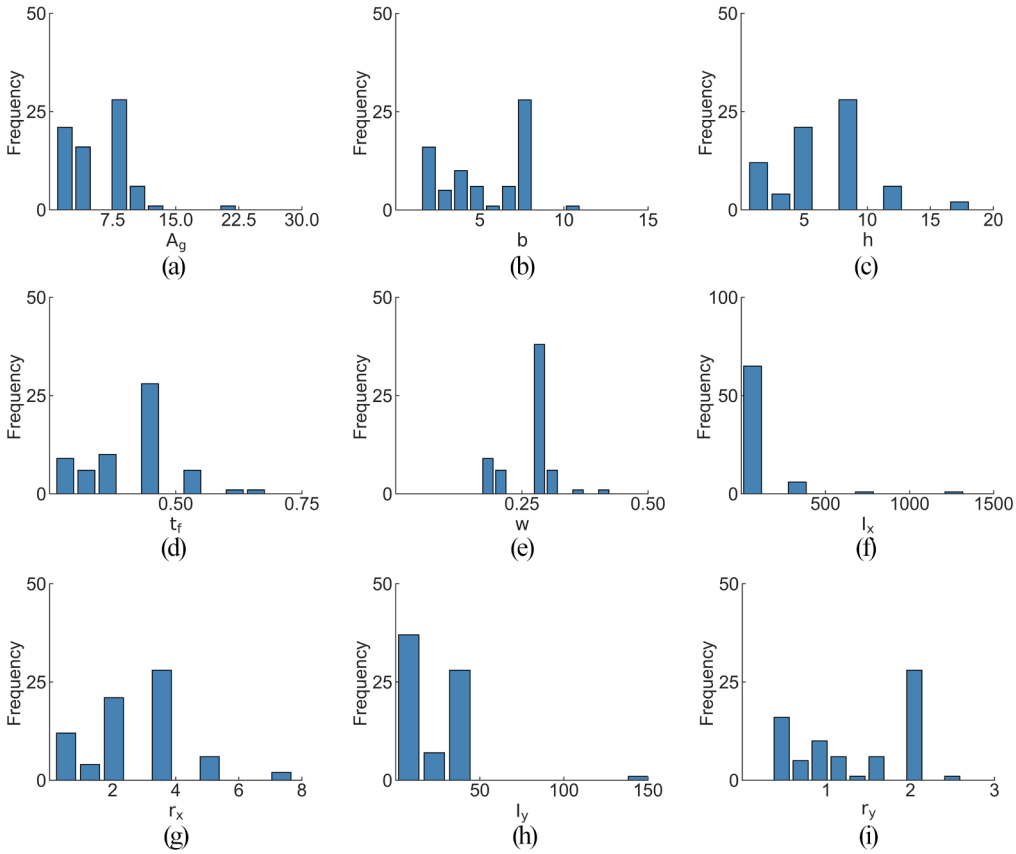

Figure 10. Distribution of the steel beam section properties: (a) A_g, (b) b, (c) h, (d) t_f, (e) w, (f) I_x, (g) r_x, (h) I_y, and (i) r_y.

- *Infill sliding and column flexural hinging* (SF): diagonal shear sliding of the infill and formation of flexural hinges in the columns;
- *Infill sliding and column shear failure* (SS): diagonal shear sliding of the infill and brittle shear failure in the columns;
- *Infill crushing and column flexural hinging* (CF): sliding in the early stages of loading and the presence of infill crushing and the formation of flexural hinges in the columns;
- *Infill crushing and column shear failure* (CS): sliding in the early stages of loading and the presence of infill crushing and brittle shear failure in the columns.

Because of the small number of specimens in the dataset with the CS failure mode, it was deemed inadequate to support the development of a data-driven model and was therefore excluded.

To develop the classification model, the dataset was randomly split into 70% for model training and hyperparameter tuning, and the remaining 30% for evaluating the performance of the machine learning models. Logistic regression (Hastie et al., 2009), decision trees (Breiman et al., 1984), random forests (Breiman, 2001), adaptive boosting (Freund and Schapire, 1997), support vector machine (Cortes and Vapnik, 1995), and multilayer

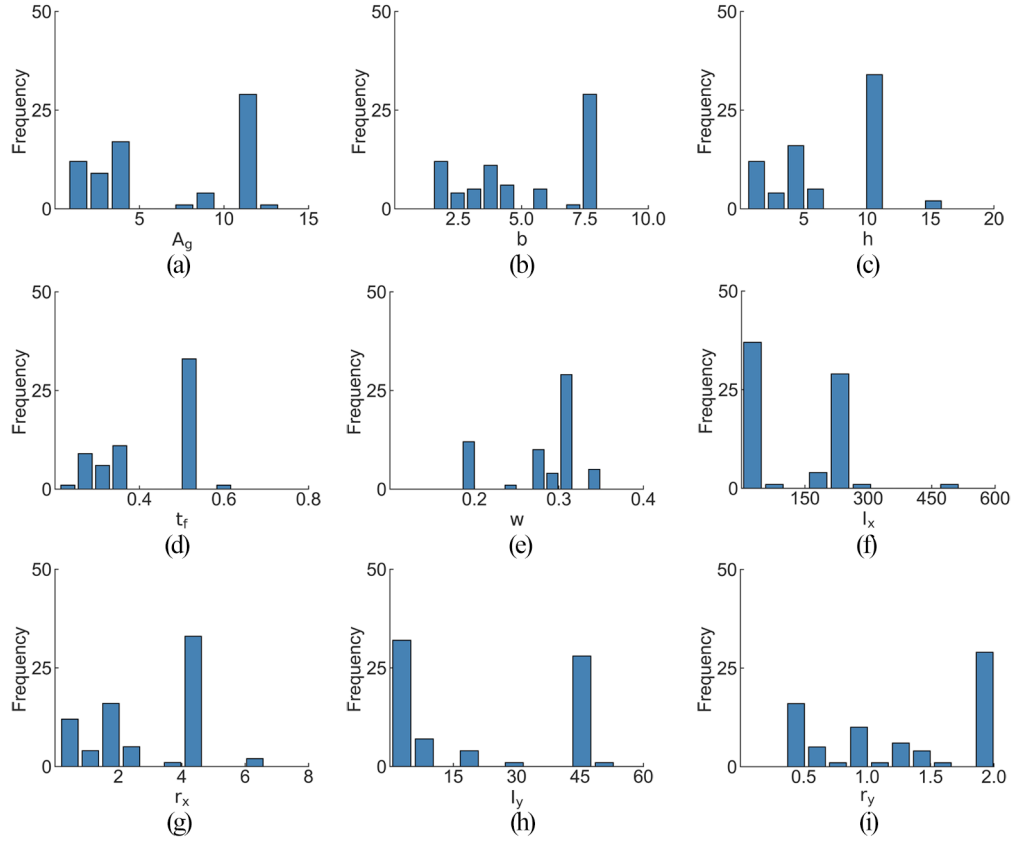

Figure 11. Distribution of the steel column section properties: (a) A_g, (b) b, (c) h, (d) t_f, (e) w, (f) I_x, (g) r_x, (h) I_y, and (i) r_y.

perceptron (Hinton, 1989) were employed for classifying the infilled frame failure modes using nine features related to the geometric and material properties. Detailed descriptions of each algorithm can be found in Huang and Burton (2019a). The machine learning models were first formulated using the training set, during which five-fold cross-validation was performed to optimize the hyperparameters. The trained models were then applied to the testing dataset, and the classification accuracies are presented in Table 11.

There are several other potential applications of the assembled database that can be undertaken in future research efforts. First, the data can be used to validate numerical models for infilled frames. Second, more empirical equations for the parameters that define the material models in OpenSees can be developed. Emphasis can be placed on the model parameters that control cyclic degradation, which are especially challenging to analyze and, as a result, have received very little attention in the research literature. Furthermore, the data for the infill panels with openings, and the infilled steel frames, which have not been utilized by the authors, can be used for various research applications.

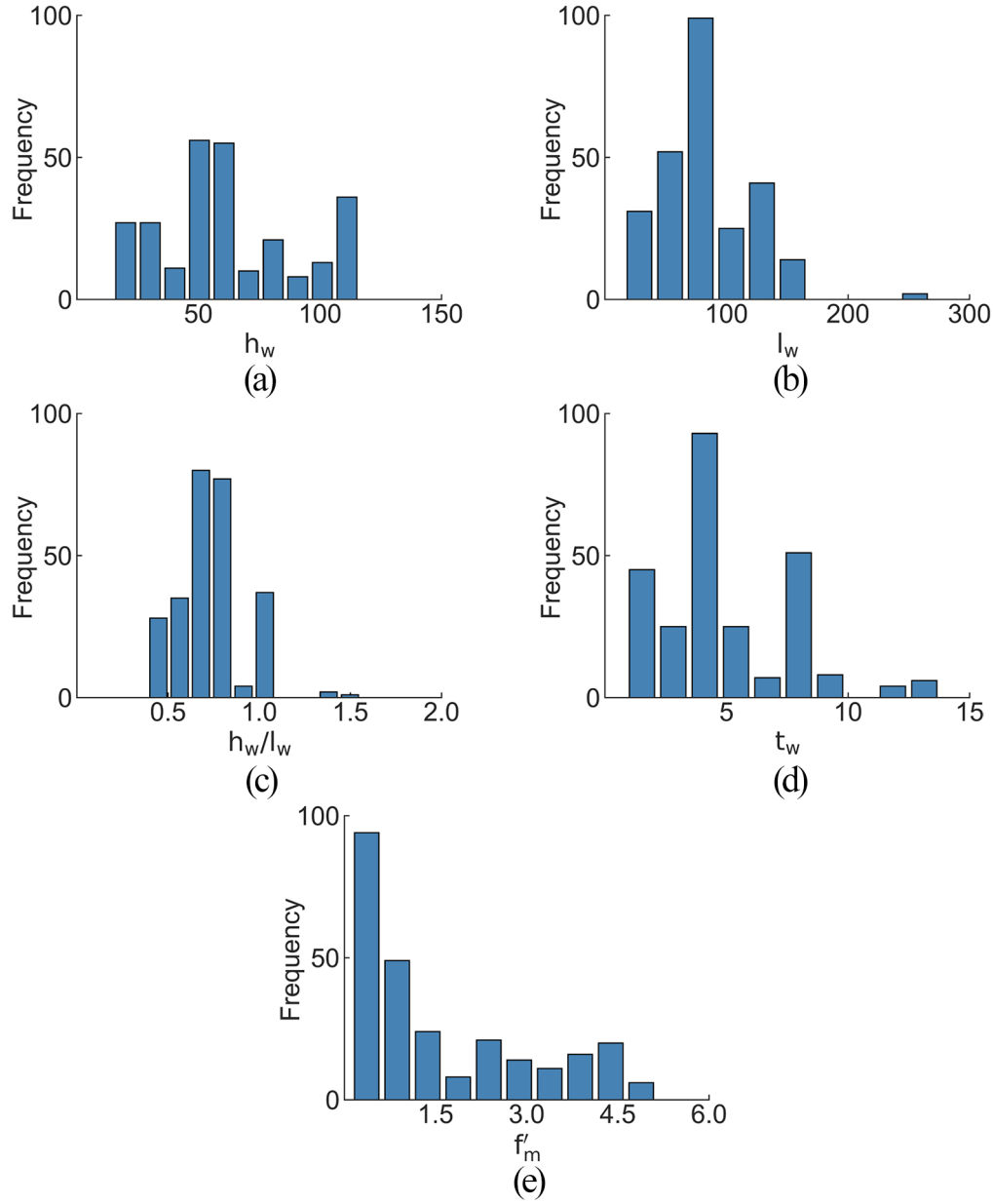

Figure 12. Distribution of the infill panel properties: (a) h_w, (b) l_w, (c) h_w/l_w, (d) t_w, and (e) f'_m.

Conclusion

A database of experiments conducted on infilled frames has been assembled and made publicly available through the DesignSafe cyberinfrastructure. In its current form, the database includes 191 infilled RC frames and 73 infilled steel frames. All the test specimens are one story, which is common for two-dimensional tests performed with pseudo-dynamic, quasi-static cyclic or monotonic loading. Among the 264 test specimens, 7 are

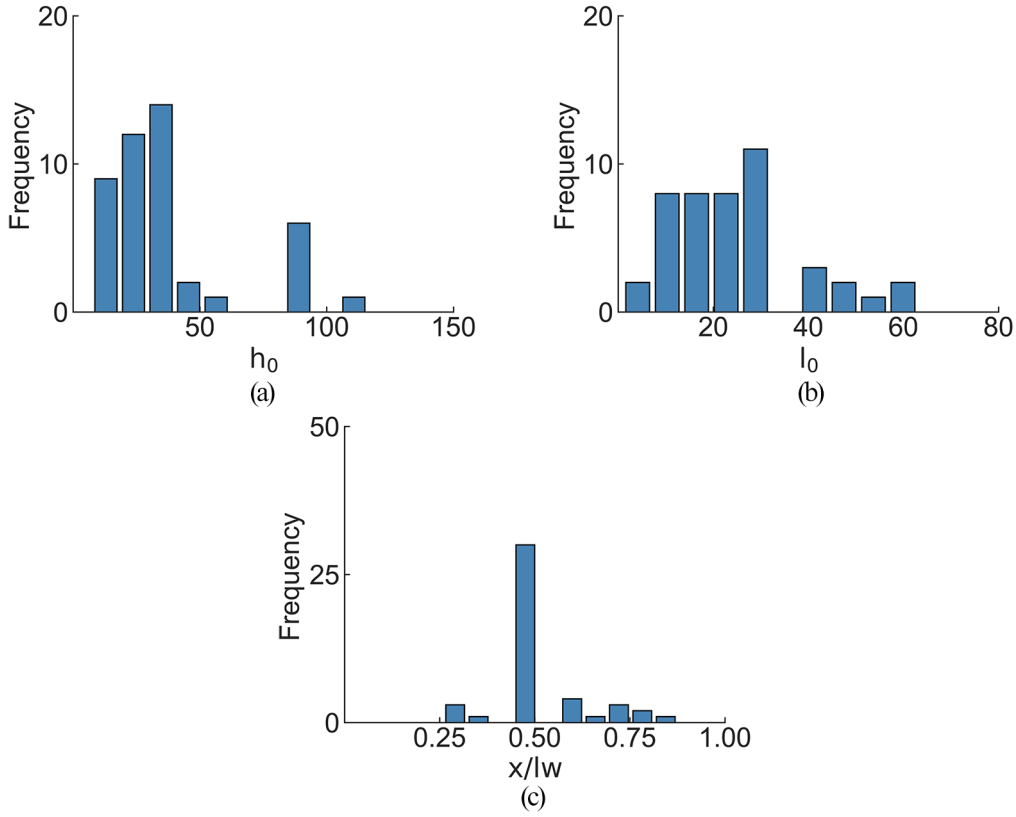

Figure 13. Distribution of the panel opening geometry: (a) h_0, (b) l_0, and (c) x/l_w.

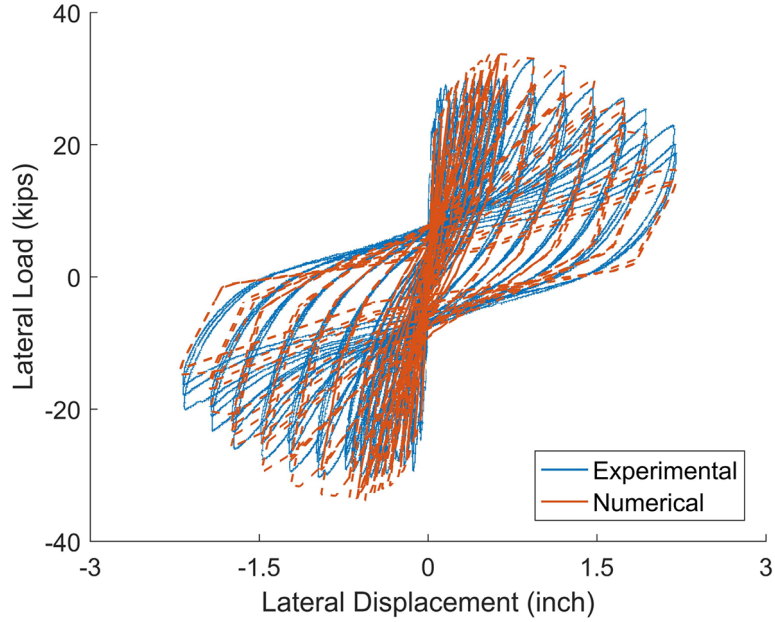

Figure 14. Calibration result for the test specimen in Bose and Rai (2014).

Table 10. Developed empirical equations

Parameter	Description	Unit	Empirical equation
K_e	Initial stiffness	kips/in	$K_e = 2.542E_m^{0.618}t_w^{0.694}\left(\frac{h_w}{l_w}\right)^{-1.096}$
F_c	Capping strength	kips	$F_c = 0.258f_m^{0.196}t_w^{0.867}l_d^{0.792}$
F_y	"Yield" strength	kips	$F_y = 0.716F_c$
F_{res}	Residual strength	kips	$F_{res} = 0.396F_c$
$\frac{d_c}{l_d}$	Axial deformation of the infill strut at peak strength (d_c) normalized by the length of the strut (l_d)		$\frac{d_c}{l_d} = 0.0105E_m^{-0.197}\left(\frac{h_w}{l_w}\right)^{0.978}$
$\frac{K_{pc}}{K_e}$	Ratio between the post-capping stiffness (K_{pc}) and the initial stiffness (K_e)		$\frac{K_{pc}}{K_e} = -0.12f_m^{-0.357}t_w^{-0.517}$

Table 11. Classification accuracy (%) for the testing dataset

	Random forest	Adaptive boosting	Decision tree	Support vector machine	Multilayer perceptron	Logistic regression
SF	93.8	93.8	87.5	100.0	81.2	68.8
SS	50.0	60.0	50.0	50.0	70.0	60.0
CF	100.0	100.0	100.0	100.0	100.0	88.9
Overall	82.9	85.7	80.0	85.7	82.9	71.4

one-story multi-bay frames and the rest are one-story one-bay frames. A variety of infill panel types are included.

The information provided in the database includes metadata, structural properties, and test results, which are valuable for studying the nonlinear behavior of infilled frames, especially the interactions between the frame and the infill panel. The database was originally assembled with the goal of calibrating material parameters for infill strut models and developing empirical equations to predict those parameters. However, various other research applications can benefit from this unified experimental database.

The current database has several limitations, which needs to be improved with additional input from the civil engineering community. Due to differences in the data quality and level of details reported in the various sources, there is missing information for several attributes of the experiments. In most instances, the force–displacement data are not available in digital format. For these cases, the figures provided for the force–displacement curves were digitized for visualization and calibration purposes. However, such data do not provide complete information on the original response and should therefore be used with caution. Finally, additional detailed information on the experiments can be found in the source paper/reports provided in the list of references.

Declaration of conflicting interests

The author(s) declared no potential conflicts of interest with respect to the research, authorship, and/or publication of this article.

Funding

The author(s) received no financial support for the research, authorship, and/or publication of this article.

References

Abdul-Kadir MR (1974) *The structural behavior of masonry infill panels in framed structures*. PhD Thesis, University of Edinburgh, Edinburgh.

ACI Committee 318 (2014) *Building Code Requirements for Structural Concrete (ACI 318-14), and Commentary (ACI 318R-14)*. Farmington Hills, MI: American Concrete Institute.

Akhoundi F, Vasconcelos G, Lourenço P, et al. (2018) In-plane behavior of cavity masonry infills and strengthening with textile reinforced mortar. *Engineering Structures* 156: 145–160.

Al-Chaar G, Issa M and Sweeney S (2002) Behavior of masonry-infilled nonductile reinforced concrete frames. *Journal of Structural Engineering* 128(8): 1055–1063.

Angel R, Abrams D, Shapiro D, et al. (1994) Behavior of reinforced concrete frames with masonry *infills*. Civil Engineering Studies SRS-589. Champaign, IL: University of Illinois at Urbana-Champaign.

Anil Altin ÖS (2007) An experimental study on reinforced concrete partially infilled frames. *Engineering Structures* 29(3): 449–460.

Asteris PG, Antoniou ST, Sophianopoulos DS, et al. (2011) Mathematical macromodeling of infilled frames: State of the art. *Journal of Structural Engineering* 137(12): 1508–1517.

ASTM A6/A6M-17a (2017) *Standard Specification for General Requirements for Rolled Structural Steel Bars, Plates, Shapes, and Sheet Piling*. West Conshohocken, PA: ASTM International.

Baran M and Sevil T (2010) Analytical and experimental studies on infilled RC frames. *International Journal of Physics and Sciences* 5(13): 1981–1998.

Basha SH and Kaushik HB (2016) Behavior and failure mechanisms of masonry-infilled RC frames (in low-rise buildings) subject to lateral loading. *Engineering Structures* 111: 233–245.

Bergami AV and Nuti C (2015) Experimental tests and global modeling of masonry infilled frames. *Earthquake and Structures* 9(2): 281–303.

Berry M, Parrish M and Eberhard M (2004) PEER structural performance database. Berkeley, CA: Pacific Earthquake Engineering Research Center.

Billington SL, Kyriakides MA, Blackard B, et al. (2009) Evaluation of a sprayable, ductile cement-based composite for the seismic retrofit of unreinforced masonry infills. In: *Improving the seismic performance of existing buildings and other structures*, San Francisco, CA, 9–11 December.

Blackard B, Willam K and Sivaselvan M (2009) *Experimental observations of masonry infilled reinforced concrete frames with openings*. *Special Publication SP-265*. Farmington Hills, MI: American Concrete Institute.

Bose S and Rai DC (2014) Behavior of AAC infilled RC frame under lateral loading. In: *Tenth U.S. national conference on earthquake engineering, frontiers of earthquake engineering*, *Anchorage, AK*, *21–25 July*.

Breiman L (2001) Random forests. *Machine Learning* 45(1): 5–32.

Breiman L, Friedman JH, Olshen RA, et al. (1984) *Classification and Regression Trees (Wadsworth Statistics/Probability)*. New York: Chapman & Hall.

Calvi GM and Bolognini D (2008) Seismic response of reinforced concrete frames infilled with weakly reinforced masonry panels. *Journal of Earthquake Engineering* 5(2): 153–185.

Campione G, Cavaleri L, Macaluso G, et al. (2014) Evaluation of infilled frames: An updated in-plane-stiffness macro-model considering the effects of vertical loads. *Bulletin of Earthquake Engineering* 13(8): 2265–2281.

Cardone D and Perrone G (2015) Developing fragility curves and loss functions for masonry infill walls. *Earthquake and Structures* 9(1): 257–279.

Chiou TC and Hwang SJ (2015) Tests on cyclic behavior of reinforced concrete frames with brick infill. *Earthquake Engineering and Structural Dynamics* 44(12): 1939–1958.

Chiozzi A and Miranda E (2017) Fragility functions for masonry infill walls with in-plane loading. *Earthquake Engineering and Structural Dynamics* 46(15): 2831–2850.

Colangelo F (2005) Pseudo-dynamic seismic response of reinforced concrete frames infilled with non-structural brick masonry. *Earthquake Engineering and Structural Dynamics* 34(10): 1219–1241.

Combescure D, Pires F, Cerqeuira P, et al. (1996) Tests on masonry infilled R/C frames and its numerical interpretation. In: *11th world conference on earthquake engineering*, Acapulco, Mexico, 23–28 June.

Cortes C and Vapnik V (1995) Support-vector networks. *Machine Learning* 20(3): 273–297.

Crisafulli FJ (1997) *Seismic behaviour of reinforced concrete structures with masonry infills*. PhD Thesis, University of Canterbury, Christchurch, New Zealand.

Da Porto F, Guidi G, Dalla Benetta M, et al. (2013) Combined in-plane/out-of-plane experimental behaviour of reinforced and strengthened infill masonry walls. In: *12th Canadian masonry symposium*, Vancouver, British Columbia, Canada, 2–5 June. Mississauga, Ontario: Canadian Masonry Design Center.

Dautaj AD, Kadiri Q and Kabashi N (2018) Experimental study on the contribution of masonry infill in the behavior of RC frame under seismic loading. *Engineering Structures* 165: 27–37.

Dawe JL and Seah CK (1989) Behaviour of masonry infilled steel frames. *Canadian Journal of Civil Engineering* 16(6): 865–876.

De Risi MT, Del Gaudio C, Ricci P, et al. (2018) In-plane behaviour and damage assessment of masonry infills with hollow clay bricks in RC frames. *Engineering Structures* 168: 257–275.

Elwood KJ (2004) Modelling failures in existing reinforced concrete columns. *Canadian Journal of Civil Engineering* 31(5): 846–859.

FEMA 306 (2000) Evaluation of Earthquake Damaged Concrete and Masonry Wall Buildings: Basic Procedures Manual. Washington, DC: The Partnership for Response and Recovery.

Fiorato AE, Sozen MA, Gamble WL, et al. (1970) An *investigation of the interaction of reinforced concrete frames with masonry filler walls. Civil Engineering Studies SRS-370*. Champaign, IL: University of Illinois Engineering Experiment Station, College of Engineering, University of Illinois at Urbana-Champaign.

Flanagan RD and Bennett RM (1999) Bidirectional behavior of structural clay tile infilled frames. *Journal of Structural Engineering* 125(3): 236–244.

Freund Y and Schapire RE (1997) A decision-theoretic generalization of on-line learning and an application to boosting. *Journal of Computer and System Sciences* 55(1): 119–139.

Gazic G and Sigmund V (2016) Cyclic testing of single-span weak frames with masonry infill. *Građevinar* 68: 617–633.

Haider S (1995) *In-plane cyclic response of reinforced concrete frames with unreinforced masonry infills*. PhD Thesis, Rice University, Houston, TX.

Haselton CB, Liel AB, Lange SL, et al. (2008) *Beam-Column Element Model Calibrated for Predicting Flexural Response Leading to Global Collapse of RC Frame Buildings*. Berkeley, CA: Pacific Earthquake Engineering Research Center.

Hastie T, Tibshirani R and Friedman J (2009) *The Elements of Statistical Learning (Springer Series in Statistics)*. New York: Springer.

Hinton GE (1989) Connectionist learning procedures. *Artificial Intelligence* 40(1–3): 185–234.

Huang H and Burton HV (2019a) Classification of in-plane failure modes for reinforced concrete frames with infills using machine learning. *Journal of Building Engineering* 25: 100767.

Huang H and Burton HV (2019b) A database of test results from steel and reinforced concrete infilled frame experiments. *Designsafe-ci*. Available at: https://doi.org/10.17603/ds2-g6t9-wx70 (accessed 8 July 2019).

Huang H, Burton HV and Sattar S (2019) Development and utilization of a database of infilled frame experiments for numerical modeling. *Journal of Structural Engineering (in press)*.

Ibarra LF, Medina RA and Krawinkler H (2005) Hysteretic models that incorporate strength and stiffness deterioration. *Earthquake Engineering and Structural Dynamics* 34(12): 1489–1511.

Kakaletsis DJ and Karayannis CG (2008) Influence of masonry strength and openings on infilled R/C frames under cycling loading. *Journal of Earthquake Engineering* 12(2): 197–221.

Kaushik HC, Rai DK, Jain S, et al. (2007) Stress-strain characteristics of clay brick masonry under uniaxial compression. *Journal of Materials in Civil Engineering* 19(9): 728–739.

Khoshnoud HR and Marsono K (2016) Experimental study of masonry infill reinforced concrete frames with and without corner openings. *Structural Engineering and Mechanics* 57(4): 641–656.

Koliou M and Filiatrault A (2017) Development of wood and steel diaphragm hysteretic connector database for performance-based earthquake engineering. *Bulletin of Earthquake Engineering* 15(10): 4319–4347.

Kumar M, Haider M and Lodi SH (2016) Response of low-quality solid concrete block infilled frames. *Proceedings of the Institution of Civil Engineers—Structures and Buildings* 169(9): 669–687.

Leuchars JM and Scrivener JC (1976) Masonry infill panels subjected to cyclic in-plane loading. *Bulletin of the New Zealand National Society for Earthquake Engineering* 9(2): 122–131.

Liberatore L, Noto F, Mollaioli F, et al. (2017) Comparative assessment of strut models for the modelling of in-plane seismic response of infill walls. In: *6th international conference on computational methods in structural dynamics and earthquake engineering*, Rhodes Island, 15–17 June, Torino, Italy: European Community on Computational Methods in Applied Sciences.

Lignos DG (2008) Sidesway collapse of deteriorating structural systems under seismic excitations. PhD Thesis, Stanford University, Stanford, CA.

Lignos DG and Krawinkler H (2011) Deterioration modeling of steel components in support of collapse prediction of steel moment frames under earthquake loading. *Journal of Structural Engineering* 137(11): 1291–1302.

Liu Y and Soon S (2012) Experimental study of concrete masonry infills bounded by steel frames. *Canadian Journal of Civil Engineering* 39(2): 180–190.

Lowes LN, Mitra N and Altoontash A (2004) A beam-column joint model for simulating the earthquake response of reinforced concrete frames. PEER Report 2003/10. Berkeley, CA: Pacific Earthquake Engineering Research Center.

Luca F, Morciano E, Perrone D, et al. (2016) MID1.0: Masonry infill RC frame experimental database. In: *Italian Concrete Days 2016*, Rome, Italy, 27–28 October. Springer International Publishing.

McKenna F, Fenves GL and Scott MH (2000) *Open System for Earthquake Engineering Simulation*. Berkeley, CA: University of California.

Mansouri A, Marefat MS and Khanmohammadi M (2014) Experimental evaluation of seismic performance of low-shear strength masonry infills with openings in reinforced concrete frames with deficient seismic details. *Structural Design of Tall and Special Buildings* 23(15): 1190–1210.

Markulak D, Radić I and Sigmund V (2013) Cyclic testing of single bay steel frames with various types of masonry infill. *Engineering Structures* 51: 267–277.

Mehrabi AB, Benson Shing P, Schuller MP, et al. (1996) Experimental evaluation of masonry-infilled RC frames. *Journal of Structural Engineering* 122(3): 228–237.

Misir IS, Ozcelik O, Girgin SC, et al. (2015) The behavior of infill walls in RC frames under combined bidirectional loading. *Journal of Earthquake Engineering* 20(4): 559–586.

Morandi P and Magenes G (2014) In-plane experimental response of strong masonry infills. In: *9th international masonry conference*, Guimarães, 7–9 July.

Mosalam KN, White R and Gergely P (1997) Static response of infilled frames using quasi-static experimentation. *Journal of Structural Engineering* 123(11). DOI: 10.1061/(ASCE)0733-9445 (1997)123:11(1462).

Noh NM, Liberatore L, Mollaioli F, et al. (2017) Modelling of masonry infilled RC frames subjected to cyclic loads: State of the art review and modelling with OpenSees. *Engineering Structures* 150: 599–621.

Pires F, Bairrão R, Campos-Costal A, et al. (1997) Behavior of masonry infilled R/C frames under horizontal loading. Experimental results. In: *11th international brick/block masonry conference*, Shanghai, China, 14–16 October.

Rathje EM, Dawson C, Padgett JE, et al. (2017) DesignSafe: New cyberinfrastructure for natural hazards engineering. *Natural Hazards Review* 18(3): 6017001.

Sassun K, Sullivan TJ, Morandi P, et al. (2016) Characterising the in-plane seismic performance of infill masonry. *Bulletin of the New Zealand Society for Earthquake Engineering* 49(1): 98–115.

Schwarz S, Hanaor A and Yankelevsky DZ (2015) Experimental response of reinforced concrete frames with AAC masonry infill walls to in-plane cyclic loading. *Structures* 3: 306–319.

Shing PB and Mehrabi AB (2002) Behaviour and analysis of masonry-infilled frames. *Progress in Structural Engineering and Materials* 4(3): 320–331.

Sigmund V and Penava D (2013) Influence of openings, with and without confinement, on cyclic response of infilled R—C frames—An experimental study. *Journal of Earthquake Engineering* 18(1): 113–146.

Stylianidis K (2012) Experimental investigation of masonry infilled R/C frames. *The Open Construction and Building Technology Journal* 6(Suppl 1-M13): 194–212.

Tasnimi AA and Mohebkhah A (2011) Investigation on the behavior of brick-infilled steel frames with openings, experimental and analytical approaches. *Engineering Structures* 33(3): 968–980.

Tawfik Essa ASA Kotp, Badr MR and El-Zanaty AH (2014) Effect of infill wall on the ductility and behavior of high strength reinforced concrete frames. *HBRC Journal* 10(3): 258–264.

Tempestti JM and Stavridis A (2017) Simplified analytical method to predict the failure pattern of infilled RC frames. In: *16th world conference on earthquake engineering*, Santiago, 9–13 January.

Tizapa SS (2009) *Experimental and numerical study of confined masonry walls under in-plane loads: Case: Guerrero State (Mexico)*. PhD Thesis, Université Paris-Est, Marne-la-Vallée.

Verderame G, Ricci P, Del Gaudio C, et al. (2016) Experimental tests on masonry infilled gravity and seismic-load designed RC frames. In: *16th international brick and block masonry conference*, Padova, 26–30 June.

Waly AA (2010) *Experimental and analytical work on the seismic performance of different types of masonry infilled reinforced concrete frames under cyclic loading*. Master's Thesis, Dokuz Eylül University, İzmir.

Yorulmaz M and Sozen M (1968) *Behavior of single-story reinforced concrete frames with filler walls*. Civil Engineering Studies SRS-337. Champaign, IL: University of Illinois at Urbana-Champaign.

Yuksel E and Teymur P (2011) Earthquake performance improvement of low rise RC buildings using high strength clay brick walls. *Bulletin of Earthquake Engineering* 9(4): 1157–1181.

Zarnic R and Tomazevic M (1985) Study of the behavior of masonry infilled reinforced concrete frames subjected to seismic loading. In: *7th international brick masonry conference*, Melbourne, Australia, 17–20 February. Brick Development Research Institute, Department of Architecture and Building, University of Melbourne.

Zhai C, Kong J, Wang X, et al. (2016) Experimental and finite element analytical investigation of seismic behavior of full-scale masonry infilled RC frames. *Journal of Earthquake Engineering* 20(7): 1171–1198.

Zovkic J, Sigmund V and Guljas I (2013) Cyclic testing of a single bay reinforced concrete frames with various types of masonry infill. *Earthquake Engineering and Structural Dynamics* 42(8): 1131–1149.